areas prevail, and four Sustainable Development Goals are predominantly in conflict with conservation of roadless areas. Maybe even more surprisingly, several of the Aichi Targets are ambivalent with respect to conserving roadless areas, rather than being in synergy entirely [six conflicting versus 11 synergistic targets (*8*); table S11].

There is an urgent need for a global strategy for the effective conservation, restoration, and monitoring of roadless areas and the ecosystems that they encompass. Governments should be encouraged to incorporate the protection of extensive roadless areas into relevant policies and other legal mechanisms, reexamine where road development conflicts with the protection of roadless areas, and avoid unnecessary and ecologically disastrous roads entirely. In addition, governments should consider road closure where doing so can promote the restoration of wildlife habitats and ecosystem functionality (*4*). Our global map of roadless areas represents a first step in this direction. During planning and evaluation of road projects, financial institutions, transport agencies, environmental nongovernmental organizations, and the engaged public should consider the identified roadless areas.

The conservation of roadless areas can be a key element in accomplishing the United Nations' Sustainable Development Goals. The extent and protection status of valuable roadless areas can serve as effective indicators to address several Sustainable Development Goals, particularly goal 15 ("Protect, restore and promote sustainable use of terrestrial ecosystems, sustainably manage forests, combat desertification, and halt and reverse land degradation and halt biodiversity loss") and goal 9 ("Build resilient infrastructure, promote inclusive and sustainable industrialization and foster innovation"). Enshrined in the protection of roadless areas should be the objective to seek and develop alternative socioeconomic models that do not rely so heavily on road infrastructure. Similarly, governments should consider how roadless areas can support the Aichi Targets (see tables S10 and S11). For instance, the target of expanding protected areas to cover 17% of the world's terrestrial surface could include a representative proportion of roadless areas.

Although we acknowledge that access to transportation is a fundamental element of human well-being, impacts of road infrastructure require a fully integrated environmental and social cost-benefits approach (*15*). Still, under current conditions and policies, limiting road expansion into roadless areas may prove to be the most cost-effective and straightforward way of achieving strategically important global biodiversity and sustainability goals.

REFERENCES AND NOTES

1. S. C. Trombulak, C. A. Frissell, *Conserv. Biol.* **14**, 18–30 (2000).
2. N. Selva *et al.*, *Environ. Manage.* **48**, 865–877 (2011).
3. W. F. Laurance, A. Balmford, *Nature* **495**, 308–309 (2013).
4. N. Selva, A. Switalski, S. Kreft, P. L. Ibisch, in *Handbook of Road Ecology*, R. van der Ree, D. J. Smith, C. Grilo, Eds. (Wiley Chichester, 2015), pp. 16–26.
5. J. Dulac, "Global land transport infrastructure requirements. Estimating road and railway infrastructure capacity and costs to 2050" (International Energy Agency, 2013).
6. W. F. Laurance *et al.*, *Curr. Biol.* **25**, R259–R262 (2015).
7. W. F. Laurance *et al.*, *Nature* **513**, 229–232 (2014).
8. Materials and methods are available as supplementary materials on *Science* Online.
9. L. Freudenberger, P. R. Hobson, M. Schluck, P. L. Ibisch, *Ecol. Complex.* **12**, 13–22 (2012).
10. E. C. Ellis, K. Klein Goldewijk, S. Siebert, D. Lightman, N. Ramankutty, *Glob. Ecol. Biogeogr.* **19**, 589–606 (2010).
11. P. W. Leadley, *et al.*, "Progress towards the Aichi Biodiversity Targets: An assessment of biodiversity trends, policy scenarios and key actions, Global Biodiversity Outlook 4 (GBO-4)" (Technical Report, Secretariat of the Convention on Biological Diversity, 2013); www.cbd.int/doc/publications/cbd-ts-78-en.pdf.
12. Convention on Biological Diversity, "Decision adopted by the Conference of the Parties to the Convention on Biological Diversity at its Tenth Meeting. X/2. The Strategic Plan for Biodiversity 2011–2020 and the Aichi Biodiversity Targets" (UN Environment Programme/Conference on Biological Diversity/Conference of the Parties, 2010); www.cbd.int/decision/cop/?id=12268.
13. D. P. Tittensor *et al.*, *Science* **346**, 241–244 (2014).
14. United Nations, "Transforming our world: The 2030 Agenda for Sustainable Development. Resolution adopted by the General Assembly (A/70/L.1)" (2015); www.un.org/ga/search/view_doc.asp?symbol=A/RES/70/1&Lang=E.
15. L. Mandle *et al.*, *Conserv. Lett.* **9**, 221–227 (2015).

ACKNOWLEDGMENTS

The data set is available through www.roadless.online and Dryad at http://dx.doi.org/10.5061/dryad.q4975. The study was funded by the Centre for Econics and Ecosystem Management at Eberswalde University for Sustainable Development, Germany; the Academy of Sciences and Literature, Mainz, Germany ("Biodiversity in Change," Nees Institute, Bonn University); and the Institute of Nature Conservation, Polish Academy of Sciences. Special thanks go to W. Barthlott for continued inspiration and support. The authors declare that they have no competing interests. P.L.I. acknowledges the research professorships "Biodiversity and natural resource management under global change" (2009–2015) and "Ecosystem-based sustainable development" (2015 onward) awarded by Eberswalde University for Sustainable Development. G.P. acknowledges funding from the European Union Framework Programme 7 project EU BON (ref. 308454). N.S. acknowledges funding from the National Science Center (DEC-2013/08/M/NZ9/00469) and the National Centre for Research and Development in Poland (Norway grants, POLNOR/198352/85/2013). P.L.I., N.S., and V.K. conceived the study. M.T.H. collected and analyzed all data, with assistance from P.L.I., L.B.-F., and G.P. P.L.I. wrote a first draft of the text and moderated its critical revision with important contributions by M.T.H., S.K., N.S., and D.A.D. All authors contributed to the interpretation of the data and critical revision of further versions. N.S., M.T.H., M.M.V., V.K., S.K., L.B.-F., and P.L.I. elaborated the supplementary materials. We appreciate the extraordinary contribution of D. Biber, who adapted Insensa-GIS to our needs. We acknowledge J. Sauermann's contributions to data processing. J.-P. Mund suggested exploring the OpenStreetMap data set. This study is part of the Roadless Areas Initiative of the Society for Conservation Biology, led by the Policy Committee of the Europe Section.

SUPPLEMENTARY MATERIALS

www.sciencemag.org/content/354/6318/1423/suppl/DC1
Materials and Methods
Figs. S1 to S11
Tables S1 to S11
Data Sources
References (*16*–*180*)

18 March 2016; accepted 16 November 2016
10.1126/science.aaf7166

PLANT PATHOLOGY

Regulation of sugar transporter activity for antibacterial defense in *Arabidopsis*

Kohji Yamada,[1,2]* Yusuke Saijo,[3,4] Hirofumi Nakagami,[5]† Yoshitaka Takano[1]*

Microbial pathogens strategically acquire metabolites from their hosts during infection. Here we show that the host can intervene to prevent such metabolite loss to pathogens. Phosphorylation-dependent regulation of sugar transport protein 13 (STP13) is required for antibacterial defense in the plant *Arabidopsis thaliana*. STP13 physically associates with the flagellin receptor flagellin-sensitive 2 (FLS2) and its co-receptor BRASSINOSTEROID INSENSITIVE 1–associated receptor kinase 1 (BAK1). BAK1 phosphorylates STP13 at threonine 485, which enhances its monosaccharide uptake activity to compete with bacteria for extracellular sugars. Limiting the availability of extracellular sugar deprives bacteria of an energy source and restricts virulence factor delivery. Our results reveal that control of sugar uptake, managed by regulation of a host sugar transporter, is a defense strategy deployed against microbial infection. Competition for sugar thus shapes host-pathogen interactions.

Plants assimilate carbon into sugar by photosynthesis, and a broad spectrum of plant-interacting microbes exploit these host sugars (*1*, *2*). In *Arabidopsis*, pathogenic bacterial infection causes the leakage of sugars to the extracellular spaces (the apoplast) (*3*), a major site of colonization by plant-infecting bacteria. Although leakage may be a consequence of membrane disintegration during pathogen infection, some bacterial pathogens promote sugar efflux to the apoplast by manipulating host plant sugar transporters (*4*, *5*). Interference with sugar absorption by bacterial and fungal pathogens reduces their virulence, highlighting a general

importance of sugar acquisition for microbial infection (*4*–*7*).

Plants control apoplastic sugar levels by sugar transporters and glycoside hydrolases. For example, sucrose exported to the apoplast is hydrolyzed to glucose and fructose by cell-wall invertases (cwINVs), which are then transported to the cytoplasm by sugar transport proteins (STPs) (*8*). Of the 14 *Arabidopsis* STP transporters, STP1 and STP13 largely govern the uptake of monosaccharides (*9*). In plant defense, STP13 contributes to resistance against the gray mold fungus *Botrytis cinerea* in *Arabidopsis* (*10*). On the contrary, the *Lr67res* mutation, which results in impaired transporter activity of LR67 (an STP13 ortholog), enhances resistance against both rust and powdery mildew fungal pathogens in wheat, although the process remains undetermined (*11*).

To investigate whether sugar uptake by STP1 and STP13 contributes to antibacterial defense in *Arabidopsis*, we spray-inoculated the phytopathogenic bacterium *Pseudomonas syringae* pv. *tomato* (*Pst*) DC3000 (*12*) onto *stp1 stp13* double-mutant plants. The plants showed increased susceptibility to *Pst* DC3000 (Fig. 1A, left) but exhibited a wild-type (WT)–like stomatal closure response (*13*) to the flg22 peptide of bacterial flagellin (fig. S1). Thus, the elevated susceptibility of *stp1 stp13* plants seems to reflect defects in their postinvasion defenses. Indeed, growth of syringe-infiltrated *Pst* DC3000 Δ*hrcC*, a less virulent strain lacking the type III secretion system (T3SS) that delivers virulence factors called effectors into plant cells, was also elevated in *stp1 stp13* plants (Fig. 1A, right). Our results suggest that STP1 and STP13 restrict bacterial proliferation in the apoplast by retrieving sugars.

To determine whether apoplastic monosaccharide levels fluctuate during antibacterial defense, we measured apoplastic glucose levels after exposure to flg22. Apoplastic glucose levels in the leaves of *stp1 stp13* plants were significantly higher than in WT plants but were indistinguishable from WT amounts in nonelicited plants (fig. S2A). Moreover, cwINV activity was comparably induced in WT and *stp1 stp13* plants in response to flg22 (fig. S2B). Together, these data indicate that STP1 and/or STP13 absorb cwINV-generated monosaccharides in the apoplast during antibacterial defense and thus perhaps significantly reduce apoplastic sugar content during bacterial challenge.

We also found that monosaccharide uptake activity in *Arabidopsis* seedlings increased after flg22 application, but not in the absence of the leucine-rich repeat receptor kinase (LRR-RK) flagellin-sensitive 2 (FLS2), the flg22 receptor in *Arabidopsis* (Fig. 1B), further suggesting that plants actively absorb sugars during antibacterial defense. Because the contribution of STP1 and STP13 to antibacterial defense implies their roles in flg22-induced monosaccharide uptake activity in *Arabidopsis* plants, we measured monosaccharide uptake in *stp1* and *stp13* plants upon mock and flg22 application. *stp1* plants retained an increase in monosaccharide uptake in response to flg22, whereas the basal activity of mock-treated plants was reduced (Fig. 1B). By contrast, *stp13* plants failed to show enhanced activity after flg22 application (Fig. 1B). This demonstrated that STP1 and STP13 contribute to basal and flg22-induced monosaccharide uptake activity, respectively. Consistent with this role of STP13, the introduction of functional STP13–green fluorescent protein (STP13-GFP) (*9*) expressed by native *STP13* regulatory DNA sequences eliminated the elevated apoplastic glucose levels of *stp1 stp13* plants in response to flg22 (fig. S2C). Nevertheless, STP1 and STP13 seem to work redundantly in antibacterial defense, given the enhanced susceptibility of *stp1 stp13* double mutants, but not *stp13* single mutants, to *Pst* DC3000 (Fig. 1A, left). STP1-mediated activity may compensate for the absence of STP13 by absorbing monosaccharide beyond the threshold required for bacterial suppression. Indeed, simultaneous loss of STP1 and STP13 caused significantly lowered monosaccharide uptake with or without flg22 application (Fig. 1B), which probably led to the enhanced susceptibility of *stp1 stp13* plants.

The STP13 dependence of flg22-induced monosaccharide uptake prompted us to explore the molecular mechanisms for regulation of STP13 activity during antibacterial defense. We found that *STP13*, but not *STP1*, expression was induced in response to flg22 (fig. S3). The abundance of STP13-GFP also rose in seedlings and mature leaves after flg22 application (Fig. 1C and fig. S4). STP13-GFP fluorescence spread at the plasma membranes of epidermal and mesophyll cells after flg22 application but was detected mainly

[1]Graduate School of Agriculture, Kyoto University, Kyoto, Japan. [2]Graduate School of Bioscience and Bioindustry, Tokushima University, Tokushima, Japan. [3]Graduate School of Biological Sciences, Nara Institute of Science and Technology, Ikoma, Japan. [4]Japan Science and Technology Agency (JST), Precursory Research for Embryonic Science and Technology (PRESTO), Kawaguchi, Japan. [5]RIKEN Center for Sustainable Resource Science, Yokohama, Japan.
***Corresponding author. Email: kohjiyamada226@gmail.com (K.Y.); ytakano@kais.kyoto-u.ac.jp (Y.T.)** †Present address: Max Planck Institute for Plant Breeding Research, Cologne, Germany.

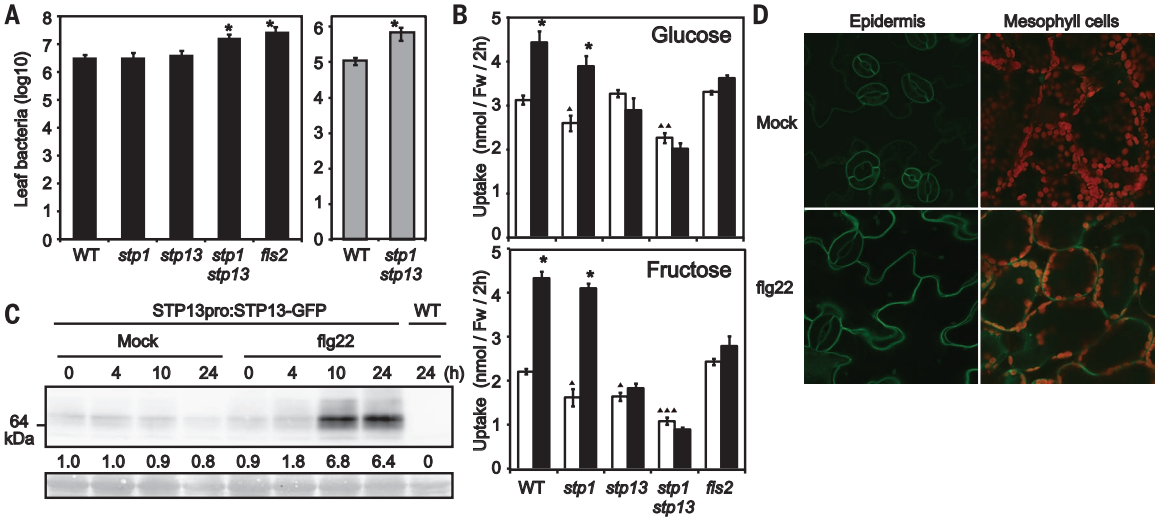

Fig. 1. Sugar transporters STP1 and STP13 contribute to antibacterial defense, and STP13 activity is induced in response to flg22. (**A**) Growth of spray-inoculated *Pst* DC3000 (black) or syringe-inoculated *Pst* DC3000 Δ*hrcC* (gray) in *Arabidopsis* leaves. Results are means ± SE, $n = 5$ biological replicates (*, $P < 0.05$ compared to the corresponding values of WT plants in two-tailed *t* tests). (**B**) ^{14}C-labeled monosaccharide uptake activity in *Arabidopsis* seedlings 24 hours after water (mock, white) or 4 μM flg22 (black) application. Results are means ± SE, $n = 3$ (*, $P < 0.05$ compared to the corresponding values of each mock treatment; ▲, $P < 0.05$, ▲▲, $P < 0.005$, ▲▲▲, $P < 0.0005$ compared to the corresponding values of mock-treated WT plants; two-tailed *t* tests). Fw, fresh weight of seedlings. (**C**) Anti-GFP immunoblot analysis for STP13-GFP in *Arabidopsis* seedlings exposed to water (mock) or 0.5 μM flg22. Numbers below the immunoblot represent relative intensities of STP13-GFP bands, normalized to backgrounds in Ponceau S-stained loading controls (bottom) and with the 0-hours mock treatment value set as 1.0. (**D**) GFP fluorescence of STP13-GFP in *Arabidopsis* seedlings exposed to water (mock) or 0.5 μM flg22 for 10 hours. Red fluorescence indicates autofluorescence of chloroplasts.

to guard cells upon mock treatment (Fig. 1D). Thus, *STP13* was transcriptionally activated during antibacterial defense.

Posttranslational modifications, including phosphorylation, can also modulate transporter activity (*14*), and to investigate such modification of STP13 during antibacterial defense, we first identified STP13-interacting proteins. The initiation of plant immunity occurs when exogenous or endogenous immune elicitors are perceived by pattern-recognition receptors (PRRs) at the plasma membrane (*15*), where STP13 is also localized. We tested whether STP13 associates with PRRs by coimmunoprecipitation (co-IP) analysis, using a transient expression system in *Nicotiana benthamiana*. STP13-FLAG coimmunoprecipitated with GFP fusions of FLS2 and two other PRRs, elongation factor–Tu receptor (EFR) and Pep receptor 1 (PEPR1), which recognize the elf18 peptide of bacterial elongation factor–Tu and the endogenous elicitor-active Pep peptides, respectively (*15*, *16*) (fig. S5), but did not coimmunoprecipitate with the GFP fusion of the plasma membrane marker protein low-temperature–inducible 6b (LTI6b) (fig. S5), indicating the specificity of STP13 interactions with these PRRs at the plasma membrane. Upon ligand perception, these PRRs associate with another LRR-RK, BRASSINOSTEROID INSENSITIVE 1–associated receptor kinase 1 (BAK1), which triggers the activation of downstream factors including the receptor-like cytoplasmic kinase botrytis-induced kinase 1 (BIK1) through trans-phosphorylation events (*15*). We found that BAK1–hemagglutinin epitope (BAK1-HA), as well as FLS2-HA, associated with STP13-FLAG in *Arabidopsis* protoplasts, whereas BIK1-HA did not (Fig. 2A). Moreover, STP13-GFP associated with FLS2 and BAK1 in mock-treated and 10-hour flg22-treated stable transgenic plants (Fig. 2B and fig S6); an FLS2-BAK1 association was also detectable 10 hours after flg22 application (fig. S7). From these interaction data, we infer that STP13 exists in complexes with FLS2 and/or BAK1, irrespective of their ligand-dependent activation states. The results suggest that STP13 participates in various PRR complexes, each of which may directly regulate STP13 activity during antibacterial defense.

We next asked whether STP13 is phosphorylated by PRR complexes in vitro. In multipass transmembrane proteins such as transporters, the longer cytoplasmic regions tend to be phosphorylated (*17*). We tested whether two STP13 fragments, the middle loop (ML, located between the sixth and seventh transmembrane domains) and the C-terminal tail (CT), expressed as glutathione *S*-transferase (GST) fusions in *Escherichia coli*, could be phosphorylated (fig. S8, A and B). A maltose-binding protein (MBP) fusion to BAK1 cytoplasmic kinase domain (CD) phosphorylated GST-STP13 CT but not GST-STP13 ML. Neither MBP-PEPR1 CD nor MBP-BIK1 phosphorylated STP13 fragments in vitro (fig. S8C). We used PEPR1 CD for this assay because FLS2 CD shows weak in vitro kinase activity (*18*). Several serine and threonine residues occur in the STP13 CT fragment (Fig. 2C, top), including the previously reported serine (S) phosphorylation site S513 (*17*). Although we substituted S513 with a non-phosphorylatable alanine (A) residue, MBP-BAK1 CD still phosphorylated GST-STP13 CT (S513A) (Fig. 2C, left). By contrast, BAK1-mediated STP13 phosphorylation was reduced by alanine substitution at threonine 485 (T485) but unaffected by alanine substitutions at S517, S523, and T524 (Fig. 2C). We concluded that BAK1 phosphorylates STP13 at T485. The corresponding residue was conserved in STP13 orthologs of other plant species (fig. S9A), but rarely among *Arabidopsis* STP homologs (fig. S9B), implying that critical and specific regulation of STP13 occurs through T485 phosphorylation in plants.

To examine whether T485 phosphorylation affects the transporter activity of STP13, we tested the function of STP13 (T485D)-GFP, in which T485 was substituted with a phosphomimic aspartic acid (D) residue. When introduced to a yeast strain deficient in multiple monosaccharide transporters, STP13 (T485D)-GFP promoted yeast growth on 10 mM glucose, more so than did STP13-GFP, although this enhancement became less clear at lower glucose concentrations (fig. S10, A and B). In addition, STP13 (T485D)-GFP yeast cells absorbed more ^{14}C-labeled monosaccharides than did STP13-GFP cells (Fig. 3A and fig. S10C). On the other hand, the T485A substitution did not affect monosaccharide uptake activity (Fig. 3A), indicating that basal sugar transport activity of STP13 is insensitive to the T485A substitution. Protein accumulation and intracellular localization of STP13 were unaffected by the T485D substitution (fig. S10, D and 0E), which suggests that the T485D substitution affects STP13 transporter activity per se. We observed a low affinity [Michaelis constant (K_m), 121.3 ± 6.3 μM] and high capacity (V_{max} value, 8.5 ± 0.6 nmol/10 min) of STP13 (T485D)-GFP cells for glucose, compared with a K_m of 71.7 ± 3.6 μM and a V_{max} of 3.3 ± 0.3 nmol/10 min of STP13 (T485A)-GFP cells (fig. S10F).

To test whether T485 phosphorylation also affects STP13 activity in planta, we measured flg22-induced glucose uptake in STP13-GFP and STP13 (T485A)-GFP plants in the *stp1 stp13* background. Although the T485A substitution did not affect STP13 activity in yeast cells or in nonelicited plants (Fig. 3, A and B), it reduced flg22-induced glucose uptake activity in plants (Fig. 3B). Protein accumulation in STP13-GFP and STP13 (T485A)-GFP plants was comparable (fig. S11). We concluded that STP13 underwent phosphorylation at T485 in response to flg22, which enhanced its sugar transport capacity. Glucose uptake in response to flg22 also increased somewhat in STP13 (T485A)-GFP plants (Fig. 3B), probably via transcriptional induction. Thus, STP13 activity is regulated at transcriptional and posttranslational levels during antibacterial defense.

We investigated the contribution of STP13 T485 phosphorylation to antibacterial defense.

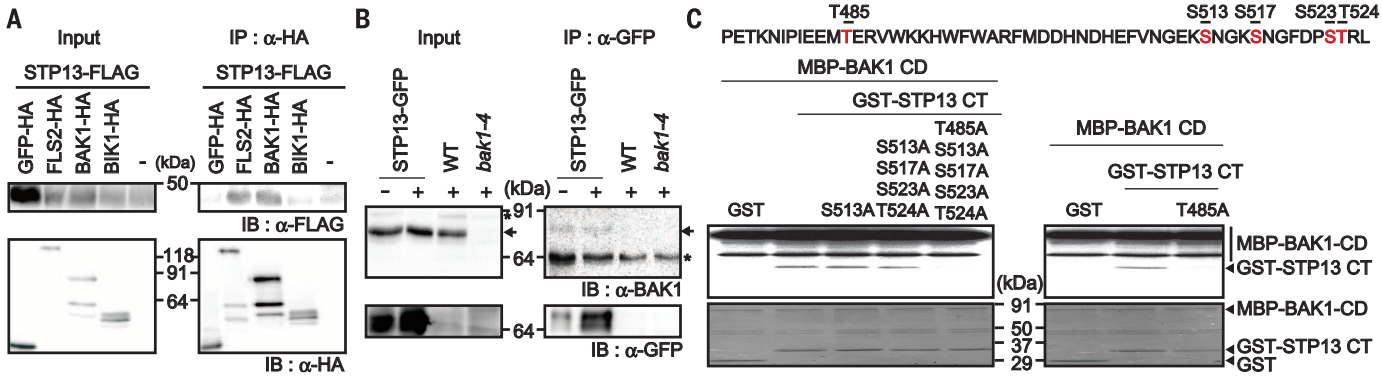

Fig. 2. STP13 participates in FLS2 complexes and is phosphorylated by BAK1. (**A** and **B**) Coimmunoprecipitation analysis between STP13 and known FLS2 complex components in *Arabidopsis* protoplasts (A) and transgenic *Arabidopsis* plants (B). + and – indicate 0.5 μM flg22 and mock treatment, respectively, for 10 hours. IP and IB denote immunoprecipitation and immunoblotting with the indicated antibodies. BAK1 (arrows) and cross-reactive bands (asterisks) are indicated. (**C**) Autoradiograph of an in vitro kinase assay. Serine and threonine residues in the STP13-CT fragment (top) are highlighted in red. Coomassie brilliant blue–stained controls are shown below.

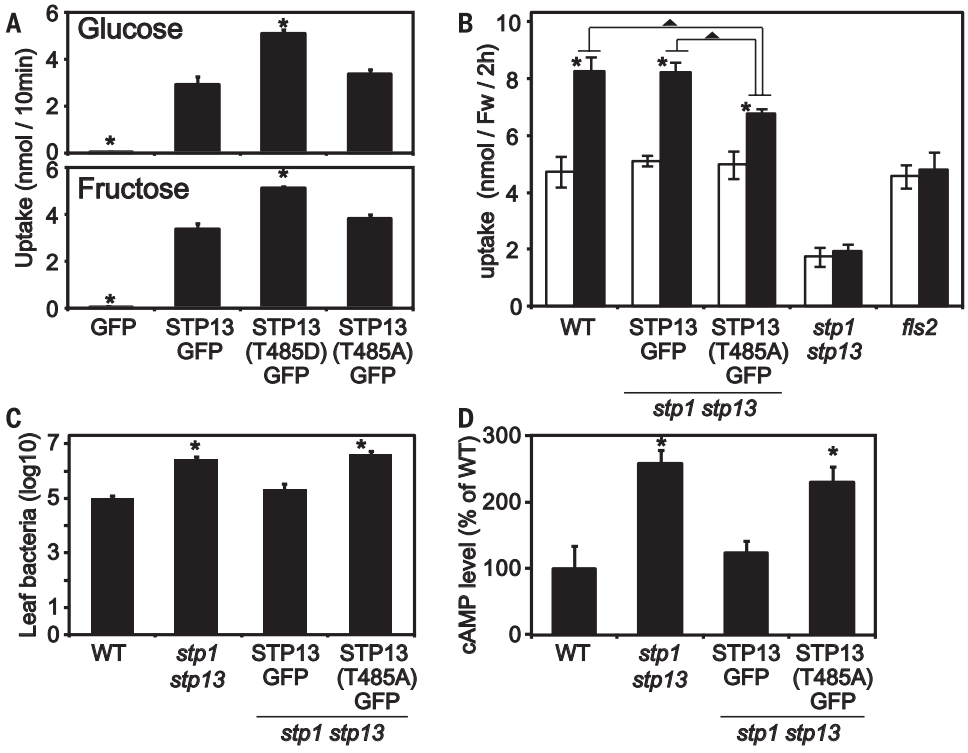

Fig. 3. Regulation of STP13 activity by T485 phosphorylation is required to suppress bacterial proliferation, partly by limiting virulence factor delivery. (**A**) ^{14}C-labeled monosaccharide uptake assay in yeast cells. Results are means ± SE, $n = 3$ (*, $P < 0.05$ in two-tailed t tests compared to the corresponding values of STP13-GFP cells). (**B**) Glucose uptake activity in *Arabidopsis* seedlings 24 hours after water (mock, white) or 4 μM flg22 (black) application. Results are means ± SE, $n = 3$ (*, $P < 0.05$, compared to the corresponding values of each mock treatment; ▲, $P < 0.05$, compared between indicated values; two-tailed t tests). (**C**) Growth of spray-inoculated *Pst* DC3000 in *Arabidopsis* leaves. Results are means ± SE, $n = 5$ (*, $P < 0.05$ compared to the values of WT plants using two-tailed t tests). (**D**) cAMP amounts in *Arabidopsis* leaves at 10 hours after spray inoculation with *Pst* DC3000 (avrPto-Cya). Results are means ± SE, $n = 4$ (*, $P < 0.05$ compared to the corresponding values of WT plants using a two-tailed t test).

Complementation of *stp1 stp13* mutant plants with STP13-GFP restored resistance to bacterial infection to WT levels (Fig. 3C), whereas the alanine-substituted version, STP13 (T485A)-GFP, was ineffective. Thus, regulation of STP13 activity through T485 phosphorylation is required for the plant to suppress bacterial proliferation.

Pathogens coordinate virulence factor expression in response to localized environments in their hosts. In the case of phytopathogenic bacteria such as *Pst* DC3000, T3SS regulatory cascades are activated via recognition of external sugars (*19*, *20*). We speculated that reduced sugar uptake activity in *stp1 stp13* plants might therefore augment bacterial effector delivery into plant cells. To test this hypothesis, we inoculated plants with bacteria expressing the T3SS effector avrPto fused to adenylate cyclase (Cya) (*21*), which produces cyclic adenosine 3′,5′-monophosphate (cAMP) only when delivered into eukaryotic cells. We observed higher cAMP levels in *stp1 stp13* plants than in WT plants, without increased bacterial growth (Fig. 3D and fig. S12), indicating elevated effector delivery in *stp1 stp13* plants. Introduction of STP13-GFP, but not STP13 (T485A)-GFP, reversed this trend (Fig. 3D). We conclude that phosphorylation-dependent regulation of STP13 activity suppresses bacterial effector delivery. The likely mechanism is that STP13 reduces sugar content in the apoplast, resulting in limited bacterial T3SS activation.

Our findings illuminate a critical role for sugar transporter regulation during bacterial challenge (fig. S13). Stimulation of STP13 activity suppresses bacterial effector delivery (Fig. 3D), thereby reducing bacterial virulence. Moreover, the elevated growth of Δ*hrcC* strain, which is defective in T3SS effector delivery, in the apoplast of *stp1 stp13* plants (Fig. 1A, right) suggests that apoplastic sugars represent an energy source for bacterial proliferation. Phytopathogenic bacteria exploit various host-derived metabolites, in addition to sugars, as energy sources or signaling molecules (*22*, *23*). Regulation of metabolite uptake upon recognition of microbial molecules may thus emerge as a key host defense strategy to restrict pathogen proliferation.

REFERENCES AND NOTES

1. R. T. Voegele, K. W. Mendgen, *Euphytica* **179**, 41–55 (2011).
2. J. Doidy *et al.*, *Trends Plant Sci.* **17**, 413–422 (2012).
3. K. Wang, M. Senthil-Kumar, C. M. Ryu, L. Kang, K. S. Mysore, *Plant Physiol.* **158**, 1789–1802 (2012).
4. L. Q. Chen *et al.*, *Nature* **468**, 527–532 (2010).
5. M. Cohn *et al.*, *Mol. Plant Microbe Interact.* **27**, 1186–1198 (2014).
6. R. Wahl, K. Wippel, S. Goos, J. Kämper, N. Sauer, *PLOS Biol.* **8**, e1000303 (2010).
7. T. Li, B. Liu, M. H. Spalding, D. P. Weeks, B. Yang, *Nat. Biotechnol.* **30**, 390–392 (2012).
8. J. S. Eom *et al.*, *Curr. Opin. Plant Biol.* **25**, 53–62 (2015).
9. K. Yamada *et al.*, *J. Biol. Chem.* **286**, 43577–43586 (2011).
10. P. Lemonnier *et al.*, *Plant Mol. Biol.* **85**, 473–484 (2014).
11. J. W. Moore *et al.*, *Nat. Genet.* **47**, 1494–1498 (2015).
12. X. F. Xin, S. Y. He, *Annu. Rev. Phytopathol.* **51**, 473–498 (2013).
13. W. Zeng, S. Y. He, *Plant Physiol.* **153**, 1188–1198 (2010).
14. K. H. Liu, Y. F. Tsay, *EMBO J.* **22**, 1005–1013 (2003).
15. D. Couto, C. Zipfel, *Nat. Rev. Immunol.* **16**, 537–552 (2016).
16. K. Yamada *et al.*, *EMBO J.* **35**, 46–61 (2016).
17. T. S. Nühse, A. Stensballe, O. N. Jensen, S. C. Peck, *Plant Cell* **16**, 2394–2405 (2004).
18. B. Schwessinger *et al.*, *PLOS Genet.* **7**, e1002046 (2011).
19. T. V. Huynh, D. Dahlbeck, B. J. Staskawicz, *Science* **245**, 1374–1377 (1989).
20. J. L. Stauber, E. Loginicheva, L. M. Schechter, *Res. Microbiol.* **163**, 531–539 (2012).
21. L. M. Schechter, K. A. Roberts, Y. Jamir, J. R. Alfano, A. Collmer, *J. Bacteriol.* **186**, 543–555 (2004).
22. A. Rico, G. M. Preston, *Mol. Plant Microbe Interact.* **21**, 269–282 (2008).
23. J. C. Anderson *et al.*, *Proc. Natl. Acad. Sci. U.S.A.* **111**, 6846–6851 (2014).

ACKNOWLEDGMENTS

We thank S. Singkaravanit-Ogawa and T. Hirase for technical support and I. Smith for critical reading. We thank K. Yamaguchi-Shinozaki, S. Tsuge, J. M. Ward, A. Reinders, and J. Mogami for published materials. This work was supported by Japan Society for the Promotion of Science KAKENHI grants (14J04880 and 16K18656, K.Y.; 15H01247, H.N.; 15H04457 and 15H05780, Y.T.), by JST PRESTO (Y.S.), and by the Asahi Glass Foundation (Y.T.). K.Y. and Y.T. conceived this study. K.Y. performed all experiments and data analyses. H.N. provided technical assistance. K.Y., Y.S., and Y.T. designed experiments and wrote the manuscript. The supplementary materials contain additional data.

SUPPLEMENTARY MATERIALS

www.sciencemag.org/content/354/6318/1427/suppl/DC1
Materials and Methods
Figs. S1 to S13
Table S1
References (*24*–*33*)

15 July 2016; accepted 11 November 2016
Published online 24 November 2016
10.1126/science.aah5692

Science

Regulation of sugar transporter activity for antibacterial defense in *Arabidopsis*

Kohji Yamada, Yusuke Saijo, Hirofumi Nakagami and Yoshitaka Takano

Science **354** (6318), 1427-1430.
DOI: 10.1126/science.aah5692originally published online November 24, 2016

Dueling for sugars

Bacteria thrive on sugar. So do plant cells. Yamada *et al.* now show how the fight for sugar plays out in the extracellular spaces around plant cells when pathogenic bacteria are invading the plant (see the Perspective by Dodds and Lagudah). In the model plant *Arabidopsis*, part of the defense response incited by the presence of pathogenic bacteria includes transcriptional and posttranscriptional regulation of sugar transporters. The resulting uptake of monosaccharides from the extracellular space makes life a little bit more difficult for the invading bacteria.

Science, this issue p. 1427; see also p. 1377